

Distribution and variability of accelerated electrons at Mars

J.S. Halekas ^{*}, D.A. Brain, R.P. Lin, J.G. Luhmann, D.L. Mitchell

Space Sciences Laboratory, 7 Gauss Way, University of California, Berkeley, CA 94720, USA

Received 20 October 2006; received in revised form 28 November 2006; accepted 16 January 2007

Abstract

We investigate accelerated electrons observed by Mars Global Surveyor (MGS), using data from the Electron Reflectometer (ER) instrument. We find three different types of accelerated electron events. Current sheet events occur over regions with weak or no crustal fields, have the highest electron energy fluxes, and are likely located on draped magnetotail fields. Extended events occur over regions with moderate crustal magnetic fields, and are most often observed on closed magnetic field lines. Localized events have the lowest energy fluxes, occur in strong magnetic cusp regions, and are the most likely kind of event to be found on open magnetic field lines. Some localized events have clear signatures of field-aligned currents; these events have much higher electron fluxes, and are preferentially observed on radially oriented open magnetic field lines. Electron acceleration events, especially localized events, are similar in many ways to events observed in the terrestrial auroral zone. However, physical processes related to those found in the terrestrial cusp and/or plasmashet could also be responsible for accelerating electrons at Mars.

© 2007 COSPAR. Published by Elsevier Ltd. All rights reserved.

Keywords: Mars; Aurora; Particle acceleration

1. Introduction

1.1. The Martian plasma environment

Unlike the Earth, Mars has no global magnetic field, though it does have strong localized crustal magnetic fields (Acuña et al., 1999). The Martian plasma environment therefore differs fundamentally from the terrestrial magnetosphere. Solar wind plasma can interact directly with the Martian atmosphere/exosphere, mass-loading the solar wind, slowing and deflecting the flow, and draping magnetic field lines around the conducting ionosphere (forming a bow shock, magnetic pileup boundary, etc.). The interaction is similar to that observed at Venus, but may be slightly perturbed over regions of strong crustal fields, where crustal fields can exclude the shocked solar wind to 1000 km altitudes or higher (Brain et al., 2003) and protect localized regions of the atmosphere from shocked solar wind plasma (Mitchell et al., 2001). Meanwhile, in magnetic cusp regions,

solar wind plasma may have direct access to the lower ionosphere along open (reconnected) magnetic field lines.

1.2. Martian aurorae

Aurorae are observed throughout the solar system, and are caused by charged particles precipitating along magnetic field lines and interacting with neutral atmospheres. Aurorae are most commonly observed at solar system bodies with global magnetic fields, though auroral emission has been observed at Venus (Phillips et al., 1986). Localized UV auroral emission was also recently observed at Mars, near a region of strong radial crustal magnetic fields (Bertaux et al., 2005), demonstrating that auroral emissions can occur in a wide variety of different plasma environments. It is an open question whether the same physical processes produce aurorae at different solar system bodies.

1.3. Accelerated electrons

At Earth, many auroral emissions are likely caused by electrons accelerated by parallel electric fields associated

^{*} Corresponding author. Tel./fax: +1 510 643 4310.

E-mail address: jazzman@ssl.berkeley.edu (J.S. Halekas).

with field-aligned current systems that couple the magnetosphere to the ionosphere (Evans, 1974; Paschmann et al., 2002). At Venus, on the other hand, auroral emissions may instead be produced by un-accelerated suprathermal electrons which precipitate directly along draped solar wind field lines that intersect the collisional atmosphere (Phillips et al., 1986). Recent observations of peaked electron and ion distributions at Mars (Brain et al., 2006a; Lundin et al., 2006a,b), possibly indicative of parallel electric field acceleration, suggest that Martian auroral physics may prove analogous to the terrestrial case. However, accelerated charged particles observed at Mars have not yet been shown to correlate directly with specific regions of auroral emission, so this question is not settled. Indeed, some recent work suggests that the Martian auroral emission may instead be caused by photoelectrons transported from the Martian day side (Leblanc et al., 2006). In any case, it is not clear how current systems analogous to those at Earth can be maintained as Mars rotates, causing constant reconfigurations of the magnetic field topology as solar wind and crustal magnetic fields interact. This suggests that Martian auroral processes, even if they do involve charged particles accelerated by parallel electric fields, may differ in other important regards from the terrestrial case.

In this paper, we investigate accelerated electrons identified by the Electron Reflectometer (ER) on the Mars Global Surveyor (MGS) spacecraft. We characterize the magnetic field morphology, electron spectra, and spatial distribution associated with three different types of accelerated electron events.

2. Electron acceleration events

2.1. Identification of accelerated electrons

We used the methodology introduced by Brain et al. (2006a) to identify accelerated electrons. The regions of observation where we searched for accelerated electrons are characterized by electron spectra that peak at energies well below 100 eV. Therefore, accelerated electrons were identified by searching all nightside MGS ER data obtained between December, 1998 and February, 2005 for electron spectra with a non-negative slope in differential flux between 100 eV and 2.5 keV (resulting in the same initial data set used in Brain et al. (2006a)). For the purposes of this paper, we selected a subset of these observations consisting of spectra which displayed a clear peak in differential flux, rather than merely a plateau. This subset of the data comprises 1338 out of the nearly 13,000 spectra originally identified by Brain et al. (2006a). The distribution of this subset in both space and time is nearly identical to that of the entire set of spectra treated in Brain et al. (2006a), so we postulate that the same physical processes are responsible for producing all of them. We focus only on this subset of data for this paper in order to concentrate on the best events, and in order to use a data set small enough to inves-

tigate each electron acceleration event individually. Due to the orbit of MGS, all of these data are located at 2 a.m. local time and ~ 400 km altitude. No attempt has been made to separate data by different solar wind conditions as done in Brain et al. (2006a).

For each of the 1338 electron spectra thus identified, we investigated the electron distributions and magnetic field characteristics of the events. Most electron acceleration events consist of more than one peaked electron spectrum; however, some are so short they consist of only a single spectrum. We conduct our analysis partly on the basis of individual spectra, partly in terms of events. We found that electron acceleration events fall into three main categories: localized acceleration events, extended acceleration events, and current sheet crossings. Though a few events were somewhat ambiguous in nature, suggesting some overlap between the three event types, we classified all the electron acceleration events into these three categories. We classified events purely based on electron characteristics, except for current sheets, which are identified on the basis of MGS magnetic field data.

2.2. Localized events

Fig. 1 shows three localized acceleration events. Localized events are identified by their brief duration (lasting

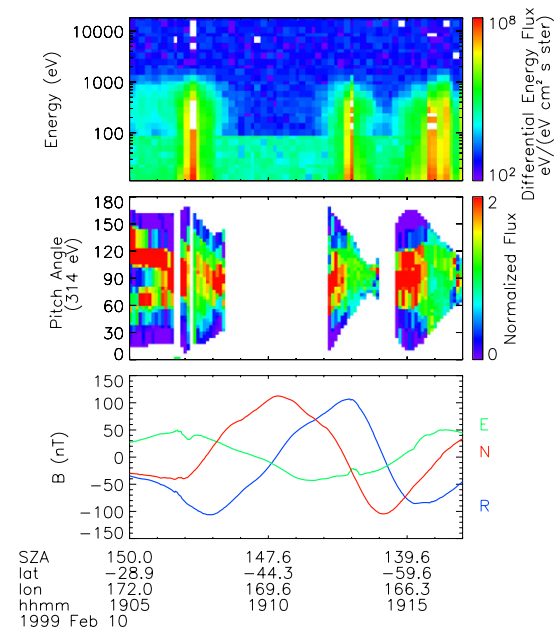


Fig. 1. Series of three localized acceleration events observed on February 10, 1999. Panels show electron differential energy flux, normalized pitch angle distributions for 314 eV electrons, and magnetic field components in local planetary coordinates. White pixels in first panel indicate no counts or instrument saturation. White pixels in second panel indicate either no pitch angle coverage or (if white for all pitch angles) time periods when the 314 eV channel is saturated or count rates are close to background (“plasma voids”). The “ledge” in the flux spectrogram during plasma voids is due to the different effective areas of the instrument for high and low electron energies, which affects the background count rate.

for only a minute or two, equivalent to a few hundred kilometer in lateral extent) and “bursty” nature, and often consist of only a few or even one peaked electron spectrum. In Fig. 1, most of the electron pitch angle distributions are two-sided loss cones indicative of closed field lines, but the localized acceleration events are associated with electrons with a one-sided loss cone distribution indicative of open field lines. This, and the association of these localized events with large radial magnetic fields, suggests that they are located in magnetic cusps.

As for the first and second event in this figure, localized events are often found associated with perturbations in the eastward component of the magnetic field. These perturbations are consistent with paired upward and downward field-aligned currents. In this figure, the first magnetic perturbation shows a fall then rise in the eastward magnetic field component, consistent with a downward current (up-going electrons) inducing a negative eastward component to the north and an upward current (down-going electrons) inducing a positive eastward component to the south, while the second indicates upward current in the north and downward in the south. In both cases shown here, and most others investigated, upward currents are roughly associated with the most intense fluxes of electrons, and with electron distributions indicative of open field lines. Downward currents, on the other hand, are associated with less intense fluxes of electrons, and with electron distributions indicative of closed magnetic field lines.

2.3. Extended events

Fig. 2 shows an extended event. Extended events last for several minutes, with lateral extents from several hundred

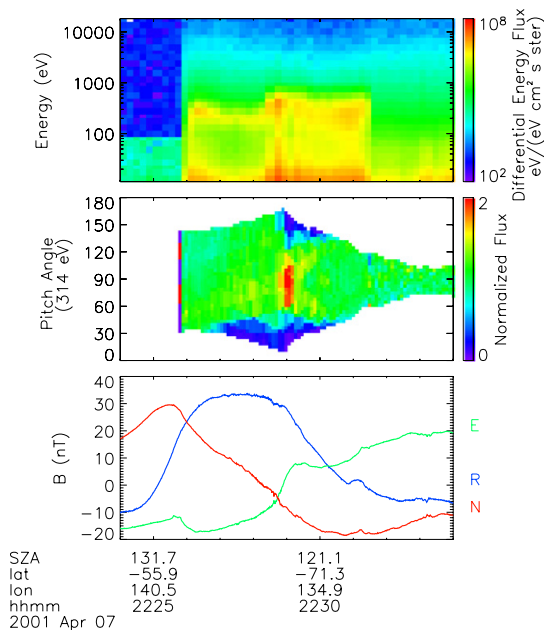


Fig. 2. Extended acceleration event observed on April 07, 2001. Panels are the same as for Fig. 1.

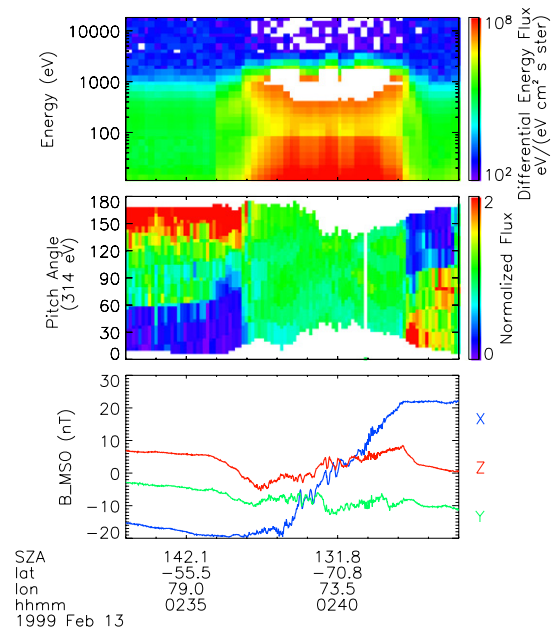


Fig. 3. Current sheet acceleration event observed on February 13, 1999. Panels are the same as for Figs. 1 and 2, except for the magnetic field, which is in MSO rather than local planetary coordinates.

kilometer up to more than a thousand kilometer. As in this example, extended events often display mixed magnetic topology. There may be perturbations in the eastward magnetic field (e.g., at 22:25:40 and 22:29:00), but they are not as clearly interpretable as field-aligned current signatures. Also, magnetic fields are not as large, and not as clearly radial, as for the localized events shown previously.

2.4. Current sheets

Fig. 3 shows a current sheet crossing. Current sheet crossings are identified by the characteristic reversal of the B_x component of the magnetic field (in MSO coordinates, analogous to GSE coordinates for Earth) and minimum in magnetic field magnitude, as in Halekas et al. (2006). Current sheet crossings are often preceded and followed by strong planet-ward flows, but distributions in the current sheet itself are sometimes more isotropic (as in this example). Current sheet crossings have the highest electron fluxes of any acceleration events.

3. Spatial distribution of electron acceleration events

The three different types of electron acceleration events identified have distinct geographical distributions, as shown in Fig. 4. Current sheets are generally located above areas with relatively weak crustal magnetic fields, away from closed field regions. Extended events are widely distributed, with a spatial distribution that broadly follows that of Martian crustal magnetic field sources. Localized events, finally, are generally found adjacent to regions of closed magnetic fields, near the boundary between open and closed topologies, and are most commonly found in

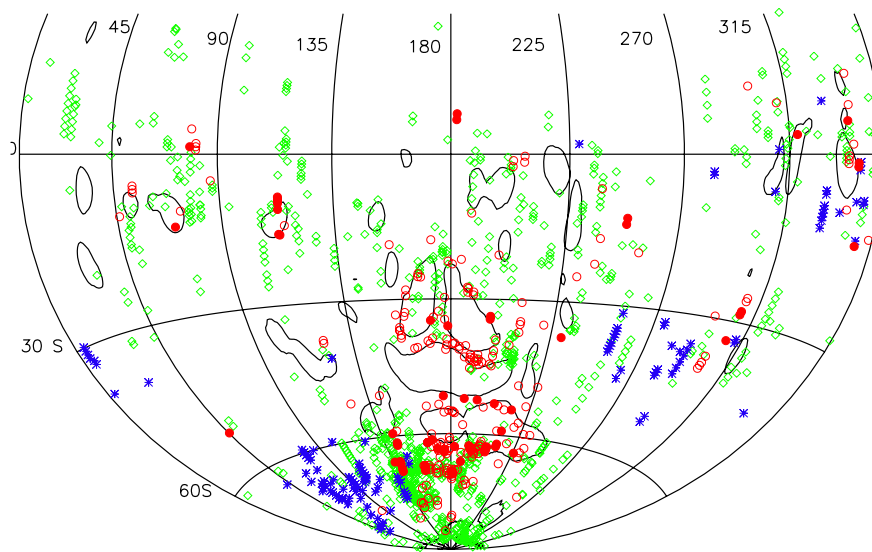


Fig. 4. Geographic locations of electron acceleration events. Blue asterisks indicate current sheets, green diamonds extended events, red circles localized events, and filled red circles localized events with clear signatures of field-aligned currents. Contours indicate the typical locations of closed magnetic field lines, inferred from electron angular distributions. (For interpretation of the references to color in this figure legend, the reader is referred to the Web version of this article.)

magnetic cusps above the strongly magnetized southern far side of Mars. Localized events which display clear indications of field-aligned currents are preferentially located in magnetic cusps in the southern part of this region, from ~ 50 to 70° S.

Though all three types of events have distinct distributions, there is significant overlap, and in some places one type of distribution melds seamlessly into another. For instance, in the southern farside region (120 – 180° E, 60 – 90° S) identified by Brain et al. (2006a), where accelerated electron distributions are particularly prevalent, there is a clear gradation from current sheets to extended events to localized events as one moves from west to east (and as magnetic field magnitude increases). This suggests the possibility that all three types of events are related and that similar physical processes may be responsible for accelerating electrons in all three types of event.

4. Characteristics of electron acceleration events

4.1. Energy flux characteristics

The electron distributions observed in each type of acceleration event have characteristic differences. For all three event types, the median energy of the peak in the spectrum is in the 217 eV energy bin of the MGS ER instrument. However, the energy flux carried by accelerated electrons differs for each type of event. The first line of Table 1 shows the median value of the differential energy flux measured at the peak of the accelerated electron distribution for each type of event. Current sheets have much higher peak differential energy fluxes than other acceleration events, while localized events have much lower fluxes. However, the subset of localized events with clear

field-aligned current signatures actually has higher fluxes than average, and much higher than other localized events. This suggests that this subset of localized events merely represent those events which have high enough differential fluxes to carry a current large enough to produce a marked perturbation in the magnetic field.

Fluxes observed in current sheets are often so large that the ER instrument is saturated (as observed in the event shown in Fig. 3). This is also the case for some other events, including the localized events shown in Fig. 1 (which are mildly saturated), but is most common for current sheets. No effort has been made to extrapolate the peak flux that would have been measured if the ER were not saturated; instead, only the peak flux value measured in energy bins where the ER is not saturated is used. Therefore, median fluxes presented here represent a lower limit on the actual median peak fluxes in the events observed.

4.2. Magnetic field characteristics

The second and third lines of Table 1 show the median magnetic field properties measured during electron acceleration events. In agreement with general trends observed in Fig. 4, current sheets occur in regions with the lowest magnetic fields (consistent with primarily external induced tail fields), extended events are associated with moderate fields consistent with a location over crustal field sources, and localized events are found in regions of strong crustal magnetic fields.

Meanwhile, extended events are associated with moderate magnetic field elevation angles consistent with primarily closed magnetic field topology. Current sheets and localized events, on the other hand, both have higher median elevation angles (more radial fields). These results in con-

Table 1
Median properties

	All	Extended	Current sheets	Localized	Localized w/field-aligned
Peak differential energy flux in eV/(eV cm ² s sr)	3.6e6	3.5e6	8.4e6	1.7e6	5.8e6
Magnetic field magnitude	27.5	26.9	18.0	49.8	49.0
Absolute value of magnetic field elevation angle	31.1	25.8	42.2	44.7	59.3

cert with those of Fig. 4 likely suggest that current sheets may be primarily associated with induced tail fields (which have a large radial component), while localized events are located near or in magnetic cusps. Localized events with field-aligned current signatures are associated with even more significantly radial magnetic fields.

4.3. Magnetic topology

It is possible to go further than general magnetic field characteristics, and look in detail at magnetic topology. We accomplish this by using electron distributions to infer the magnetic topology. For example, one-sided loss-cone distributions are consistent with open magnetic field lines (or field lines draped through the collisional atmosphere) and two-sided loss-cone distributions are consistent with closed magnetic field lines. Other distributions, such as counter-streaming electrons, do not clearly correspond to a specific type of magnetic topology. Brain et al. (in preparation) have developed a method for using electron distributions to determine magnetic topology in this manner in an automated fashion. We use this method, and classify all accelerated electrons according to their magnetic topology; the results of this analysis are shown in Table 2. The technique can only be applied when the ER is oriented such that the range of pitch angles measured is large enough to resolve the loss cone, the magnetic field is large enough that uncertainties in the magnetic field direction are small, and the electron distribution is not contaminated by sunlight or other effects. Because of these restrictions, many events cannot be classified according to magnetic topology. It is also important to note that, if parallel electric fields are present, they may affect the electron distributions; however, the determination of the presence or absence of loss cones is still possible.

We find that the majority of accelerated electrons (those whose topology can be determined) are associated with two-sided loss cone distributions. Other common types of distributions are one-sided loss cones and counter-stream-

ing distributions. A variety of other types of distributions each comprise less than 2% of the observations.

Fewer current sheets can be classified in terms of topology, because they occur in weak magnetic field regions. However, for cases that can be classified, closed topology is much less likely and counter-streaming distributions much more common than for any other type of event. This is consistent with the expected association of current sheets with draped (induced) magnetotail fields.

Proportionally more of the localized events can be classified by magnetic topology, because they occur in regions of strong magnetic fields. Localized events are also much more likely to occur on open magnetic fields, consistent with a location near or in magnetic cusps. Localized events with field-aligned current signatures are even more likely to be on open magnetic field lines. All of these results are consistent with what one would expect from the general magnetic field characteristics reported above.

We conducted χ^2 -tests to determine the significance of the differences in topology we found. We found that the distribution of different types of topology associated with extended events is statistically indistinguishable from the data set as a whole, as expected since they comprise the largest fraction of the data set. Current sheets and localized events, on the other hand, have statistically significantly different distributions of different types of topologies from the data set as a whole and from extended events. There is less than a 0.001% chance that the current sheets or localized events are drawn from the same distribution of topologies as the full data set or the extended events. The differences between localized events with field-aligned current signatures and all localized events, while interesting, comprise too few observations to be highly statistically significant.

The fact that localized acceleration events, which are most analogous to observations in the terrestrial auroral zone, are more often associated with open magnetic field lines, has interesting implications. A closed current system like that postulated to drive parallel electric fields

Table 2
Topology

	All	Extended	Current sheets	Localized	Localized w/field-aligned
Total	1338	954	126	258	62
Unclassifiable	576 (43%)	440 (46%)	71 (56%)	65 (25%)	13 (21%)
Closed	415 (31%)	296 (31%)	9 (7%)	110 (43%)	18 (29%)
Open	172 (13%)	98 (10%)	18 (14%)	56 (22%)	21 (34%)
Counter-streaming	29 (2%)	17 (2%)	10 (8%)	2 (1%)	1 (2%)
Other	146 (11%)	103 (11%)	18 (14%)	25 (10%)	9 (15%)

in the terrestrial auroral zone should lie on closed magnetic field lines. One possibility is that the electrons we observe on open field lines were accelerated on closed field lines, but have since drifted or been scattered onto open field lines.

Finally, it is worth noting that accelerated electrons observed at Mars may be much more analogous to those observed in the terrestrial cusp than those in the terrestrial auroral zone. Pfaff et al. (1998) found many similar features in this region, including accelerated ion and electron distributions indicative of parallel electric field acceleration and tangential magnetic field perturbations indicative of field-aligned currents. Electron distributions were found to be similar to those observed in the terrestrial auroral zone, but generally peaked at lower energies of a few hundred eV. They postulated that parallel electric fields are produced by the interaction between ionospheric plasma and precipitating magnetosheath particles. It is very likely that similar processes could operate in the Martian system. If Martian accelerated electrons are analogous to accelerated electrons in the terrestrial cusp, the results of Pfaff et al. (1998) suggest that they may be observed in association with injections of precipitating high-energy magnetosheath ions. This represents an avenue for further study, especially if MEX and MGS data can be used in concert.

5. Conclusions

We find that accelerated electron events at Mars consist of three types; current sheets, localized events, and extended events. Current sheets occur over regions of weak crustal fields, have the highest electron energy fluxes, and are most often associated with one-sided loss cone distributions or counter-streaming electrons. Extended events occur over regions with crustal magnetic fields, and are most likely to be observed on closed magnetic field lines. Localized events have the lowest energy fluxes, occur in strong magnetic cusp regions, and are the most likely kind of event to be found on open magnetic field lines. Some localized events have clear signatures of field-aligned currents; these events have much higher electron fluxes, and are preferentially observed on radially oriented open magnetic field lines. The distributions of these three types of event overlap and sometimes gradually merge together, possibly suggesting a common or related origin. However, current sheet events are consistent with an occurrence on draped magnetotail fields (suggesting acceleration process-

es analogous to those observed in the terrestrial plasma-sheet), while localized events (especially those with field-aligned current signatures) are similar in many ways to those observed in the terrestrial auroral zone. On the other hand, localized events are also similar to events observed in the terrestrial cusp, suggesting that cusp physics may be at least as relevant as auroral physics. Whatever the origin of accelerated electrons at Mars, it is clear that we will have to understand the whole coupled system of solar wind, induced magnetosphere, and ionosphere in order to fully characterize them.

References

- Acuña, M.H., Connerney, J.E.P., Ness, N.F., et al. Global distribution of crustal magnetization discovered by the Mars Global Surveyor MAG/ER experiment. *Science* 284, 790–793, 1999.
- Bertaux, J.-L., Leblanc, F., Witasse, O., et al. Discovery of an aurora on Mars. *Nature* 435, 790–794, doi:10.1038/nature03603, 2005.
- Brain, D.A., Bagenal, F., Acuña, M.H., Connerney, J.E.P. Martian magnetic morphology: contributions from the solar wind and crust. *J. Geophys. Res.* 108, 1424, doi:10.1029/2002JA009482, 2003.
- Brain, D.A., Halekas, J.S., Peticolas, L.M., et al. On the origin of aurorae on Mars. *Geophys. Res. Lett.* 33, L01201, doi:10.1029/2005GL024782, 2006a.
- Brain, D.A., Lillis, R.J., Halekas, J.S., Mitchell, D.L., Lin, R.P. Pitch angle distributions as indicators of magnetic field topology near Mars. *J. Geophys. Res.*, in preparation.
- Evans, D.S. Precipitating electron fluxes formed by a magnetic field aligned potential difference. *J. Geophys. Res.* 79, 2853, 1974.
- Halekas, J.S., Brain, D.A., Lillis, R.J., et al. Current sheets at low altitudes in the Martian magnetotail. *Geophys. Res. Lett.* 33, L13101, doi:10.1029/2006GL026229, 2006.
- Leblanc, F., Witasse, O., Winningham, J., et al. Origins of the Martian aurora observed by Spectroscopy for Investigation of Characteristics of the Atmosphere of Mars (SPICAM) on board Mars Express. *J. Geophys. Res.* 111, A09313, doi:10.1029/2006JA011763, 2006.
- Lundin, R., Winningham, D., Barabash, S., et al. Plasma acceleration above Martian magnetic anomalies. *Science* 311, 980–983, doi:10.1126/science.1122071, 2006a.
- Lundin, R., Winningham, D., Barabash, S., et al. Ionospheric plasma acceleration at Mars: ASPERA-3 results. *Icarus* 182, 308–319, 2006b.
- Mitchell, D.L., Lin, R.P., Mazelle, C., et al. Probing Mars' crustal magnetic field and ionosphere with the MGS Electron Reflectometer. *J. Geophys. Res.* 106, 23419–23427, 2001.
- Paschmann, G., Haaland, S., Treumann, R. (Eds.). *Auroral plasma physics* Space Sci. Rev. 1–4, 2002.
- Pfaff, R., Clemmons, J., Carlson, C., et al. Initial FAST observations of acceleration processes in the cusp. *Geophys. Res. Lett.* 25, 2037–2040, 1998.
- Phillips, J.L., Luhmann, J.G., Stewart, A.I.F. The Venus ultraviolet aurora – observations at 130.4 nm. *Geophys. Res. Lett.* 13, 1047–1050, 1986.